Chin. J. Astron. Astrophys. Vol. 6 (2006), **Suppl. 2**, 105–112
(*http://www.chjaa.org*)

Chinese Journal of
Astronomy and
Astrophysics

Drifting Subpulse Phenomenon in Pulsars

Janusz Gil[1,2 ⋆], George Melikidze[1,3] and Bing Zhang[2]

[1] Institute of Astronomy, University of Zielona Góra, Lubuska 2, 65-265, Zielona Góra, Poland
[2] Department of Physics,University of Nevada Las Vegas, Las Vegas, NV, USA
[3] Abasumani Astrophysical Observatory, Al. Kazbegi ave. 2a, 0160, Tbilisi, Georgia

Abstract The problem of formation of a partially screened inner acceleration region for 102 pulsars with drifting subpulses is considered. It is argued by means of the condition $T_{\rm c}/T_{\rm s} > 1$ (where $T_{\rm c}$ is the critical temperature above which the surface delivers thermal flow at the corotation limited level and $T_{\rm s}$ is the actual surface temperature) that an efficient acceleration region can be formed in a very strong and curved, non-dipolar surface magnetic field, even exceeding 10^{14} G in general. Both positively and negatively charged polar caps are considered. Also, both curvature radiation as well as resonant inverse Compton radiation seed photons are taken into account. It is argued that the former mechanism is much more likely to account for the sparking discharge of the partially screened inner acceleration region in pulsars.

Key words: pulsars: drifting subpulses — radio emission — X-ray thermal radiation

1 INTRODUCTION

The phenomenon of drifting subpulses has been widely regarded as a powerful tool for the investigation of mechanisms of pulsar radio emission. First and still very popular physical explanation of this phenomenon has been proposed by Ruderman & Sutherland (1975). Their model was successful compared with a few cases of pulsars with drifting subpulses known at that time. Rankin (1986) compiled a list of about 40 cases, including division into core and conal components. At that time drifting subpulses could still be regarded as some kind of exceptional phenomenon. However recently, Weltevrede, Edwards & Stappers (2005) presented the results of a systematic, unbiased search for subpulse modulation in 187 pulsars and found that the fraction of pulsars showing drifting subpulse phenomenon is likely to be larger than 55% (see also these Proceedings). The authors concluded that the conditions required for drifting mechanism to work cannot be very different from the emission mechanism of radio pulsars. WES05 suggest that the subpulse drifting phenomenon in an intrinsic property of the emission mechanism, although drifting could in some cases be very difficult or even impossible to detect due to low signal to noise ratio.

The classical vacuum gap model of RS75, in which sparks-associate sub-beams of subpulse emission circulate around the magnetic axis due to $\boldsymbol{E} \times \boldsymbol{B}$ drift of spark plasma filaments, provides the most natural and plausible explanation of drifting subpulse phenomenon. However, despite its popularity, it suffers from the well known binding energy problem. Recently Gil & Mitra (2001) revisited this problem and found that the formation of vacuum gap (VG) is in principle possible, although it requires a very strong surface magnetic fields, much stronger than a dipolar components inferred from the observed spindown rate. In other words, GM01 concluded that in general, the surface magnetic field at the polar cap must be significantly nondipolar. It seems that there is a growing observational evidence of such nondipolar structures of surface magnetic field (e.g. Urpin & Gil 2004). Gil & Melikidze (2002) developed further this idea and calculated the VG model for 42 pulsars tabulated by R86. Using different pair production mechanisms and different

⋆ E-mail: jag@astro.ia.uz.zgora.pl

available estimates of the cohesive energy of surface iron ions, GM02 demonstrated that VG can be form for all pulsars from R86. They concluded that the resonant inverse Compton scattering (ICS) seed photons driving the spark discharges were strongly preferred, while the curvature radiation (CR) seed photons were unable to operate efficiently in general.

Gil, Melikidze & Geppert (2003) developed further the idea of the inner acceleration region above the polar cap by including the partial screening by thermal flow from the surface heated by sparks. They succeeded to construct a self-consistent model, which they applied to a number of well known drifters. In this paper we apply the partially screened inner acceleration model to a new set of 102 pulsars from WES05 and show that it can work in every case, provided that the surface non-dipolar magnetic field is strong enough, even stronger than suggested by GM01 and GM02. Moreover, the ICS mechanism is no longer preferred and CR dominated discharge seems even better suited. The thermostatic regulation sets the surface temperature at the level of few MK, which is consistent with recent XMM-Newton observations of drifting subpulse pulsar B0943+10 performed and analyzed by Zhang, Sanwal & Pavlov (2005).

2 CHARGE DEPLETED INNER ACCELERATION REGION

The inner acceleration region above the polar cap results from the deviation of a local charge density ρ from the co-rotational charge density (GJ69) $\rho_{\rm GJ} = -\boldsymbol{\Omega}\cdot\boldsymbol{B}_{\rm s}/2\pi c \approx \pm B_{\rm s}/cP$, where the positive/negative sign corresponds to $^{56}_{26}$Fe ions/electrons, for antiparallel and parallel relative orientation of magnetic and spin axes, respectively. As already mentioned in the Introduction, more and more evidence exists both observational and theoretical (see Urpin & Gil 2004 and references therein) that the actual surface magnetic field $B_{\rm s}$ is highly non-dipolar. Its magnitude can be described in the form $B_{\rm s} = bB_{\rm d}$ (Gil & Sendyk 2000), where the enhancement coefficient $b > 1$ and $B_{\rm d} = 2\times10^{12}(P\dot{P}_{-15})^{1/2}$ G is the canonical, star centered dipolar magnetic field, P is the pulsar period and $\dot{P}_{-15} = \dot{P}/10^{-15}$ is the period derivative.

The polar cap is defined as the locus of magnetic field lines that penetrate the so-called light cylinder (GJ69). In general case, the polar cap radius can be written as $r_{\rm p} = b^{-0.5}1.45\times10^4 P^{-0.5}$ cm (GS00), where the factor $b^{-0.5}$ describes squeezing of the dipolar polar cap area due to the magnetic flux conservation. One should realize, however, that the polar cap radius $r_{\rm p}$ expressed by the above equation is only a characteristic dimension of the region above which a high accelerating potential drop can develop. In fact, the actual polar cap can be largely deformed from circularity in the presence of strong nondipolar surface magnetic field.

As mentioned in the Introduction, the charge depletion above the polar cap, traditionally called vacuum gap (VG), can result from bounding of the positive $^{56}_{26}$Fe ions (at least partially) in the neutron star surface. If this is possible, then positive charges cannot be supplied at the rate that would compensate the inertial outflow through the light cylinder. As a result, a significant part of the unipolar potential drop (GJ69, RS75) develops above the polar cap, which can accelerate charge particles to relativistic energies and power the pulsar radiation mechanism. The characteristic height h of such an acceleration region is determined by the mean free path of pair producing high energy photons. In other words, the growth of the accelerating potential drop is limited by the avalanche production of electron-positron plasma (e.g. RS75, CR80). The accelerated positrons will leave the acceleration region, while the electrons will bombard the polar cap surface, causing a thermal ejection of ions, that could be otherwise bound in the surface in the absence of additional heating. This thermal ejection will cause a partial screening of the acceleration potential drop ΔV corresponding to a shielding factor $\eta = 1-\rho_i/\rho_{\rm GJ}$, where ρ_i is thermonically ejected charge density and $\Delta V = \eta 2\pi/cPB_{\rm s}h^2$, where $B_{\rm s}$ is defined by above equation and h is the model dependent height (see below) of the acceleration region. Two VG models can be considered under the near-threshold (NT) condition valid for strong surface magnetic field $B_{\rm s} > 0.1B_{\rm q}$, where $B_{\rm q} = 4.414\times10^{13}$ G is the so-called quantum magnetic field (RS75 and references therein): Curvature Radiation dominated Near Threshold Partially Screened Gap (CR-NTPSG) model and Inverse Compton Scattering dominated Near Threshold Partially Screened Gap (ICS-NTPSG) model, in which the potential drop is limited by the curvature radiation (CR) and the resonant inverse Compton scattering (ICS) seed photons, respectively (for details see GM01, GM02, GMG03 and references therein). In the strong surface magnetic field $B_{\rm s} > 5\times10^{12}$ G the high energy photons with energy $E_f = \hbar\omega$ produce electron-positron pairs at or near the kinematic threshold $\hbar\omega = 2mc^2/\sin\theta$, where $\sin\theta = l_{\rm ph}/\mathcal{R}$, $l_{\rm ph}$ is the photon mean free path for pair formation and $\mathcal{R} = \mathcal{R}_6\times10^6$ cm is the radius of curvature of magnetic field lines.

2.1 CR-NTPSG Model

In this model the cascading e^-e^+ pair plasma production is driven (or at least dominated) by the curvature radiation photons with typical energy $\hbar\omega = (3/2)\hbar\gamma^3 c/\mathcal{R}$. where γ is the typical Lorentz factor of electrons/positrons moving relativistically along surface magnetic field lines with a radius of curvature $\mathcal{R}$. In the quasi-steady conditions the height h of the acceleration region is determined by the mean free path $l_{\rm ph}$ for pair production by energetic CR photon in strong and curved magnetic field. Following GM01 and GM02 and including partial screening (GMG03) we obtain

$$h \approx h^{\rm CR} = (3.1\times 10^3)\mathcal{R}_6^{2/7}\eta^{-3/7}b^{-3/7}P^{3/14}\dot{P}_{-15}^{-3/14}\ {\rm cm}. \quad (1)$$

2.2 ICS-NTPSG Model

In this model the cascading pair plasma production is driven (or at least dominated) by the resonant inverse Compton scattering, with typical photon energy $\hbar\omega = 2\gamma\hbar e B_{\rm s}/mc$. In the quasi-steady conditions the height h of the acceleration region is determined by the condition $h = l_{\rm ph} \sim l_{\rm e}$. Here $l_{\rm ph}$ is the mean free path of the ICS photon to pair produce and $l_{\rm e} = 0.0027\gamma^2(B_{\rm s}/10^{12}\,{\rm G})^{-1}(T_{\rm s}/10^6\,{\rm K})^{-1}$ is the mean free path of the electron to emit this high energy ICS photon (ZHM00), where $B_{\rm s}$ is the surface magnetic field and $T_{\rm s}$ is the actual surface temperature. Following GM01 and including partial screening (GMG03) we obtain

$$h \approx h^{\rm ICS} = (5.3\times 10^3)\mathcal{R}_6^{0.57}\eta^{-0.14}b^{-1}P^{-0.36}\dot{P}_{-15}^{-0.5}\ {\rm cm}. \quad (2)$$

In the above equations $\mathcal{R}_6 = \mathcal{R}/10^6$ cm is normalized curvature radius of the surface magnetic field lines. For simplicity, in the following discussion the above equations will be referred as to CR and ICS cases, respectively.

3 BINDING ENERGY PROBLEM

If the binding energy of $^{56}_{26}$Fe ions is large enough to prevent thermionic emission, a charge depleted acceleration region can form just above the polar cap. Normally, at the solid-vacuum interface, the charge density of outflowing ions is roughly comparable with density of the solid at the surface temperature $kT_{\rm s} = \varepsilon_{\rm c}$, where $\varepsilon_{\rm c}$ is the cohesive (binding) energy and $k = 8.6\times 10^{-8}$ keV K^{-1} is the Boltzman constant. However, in case of pulsars, only the corotational charge density $\rho_{\rm GJ}$ can be reached, and the $^{56}_{24}$Fe ion number density corresponding to $\rho_{\rm GJ}$ is about $\exp(-30)$ times lower than in the neutron star crust. Since the density of outflowing ions ρ_i decreases in proposition to $\exp(-\varepsilon_{\rm c}/kT_{\rm s})$, then one can write $\rho_i/\rho_{\rm GJ} \approx \exp(30 - \varepsilon/kT_{\rm s})$. At the critical temperature $T_i = \varepsilon_{\rm c}/30k$ the ion outflow reaches the maximum value $\rho = \rho_{\rm GJ}$, and the numerical coefficient 30 is determined from the tail of the exponential function with an accuracy of about 10%.

Calculations of binding energies are difficult and uncertain (see Lai 2001 for review and critical discussion). In this paper we will use the results of Jones (1986), which were recommended by Lai (2001) in his review paper. J86 obtained $\varepsilon_{\rm c}$=0.29, 0.60 and 0.92 keV for $B_{\rm s} = 2, 5$ and 10×10^{12} G, respectively. These values can be approximately represented by the function $\varepsilon_c \simeq (0.18\,{\rm keV})(B_{\rm s}/10^{12})^{0.7}$ G and converted into critical ion temperature

$$T_i \simeq (0.7\times 10^5\,{\rm K})(B_{\rm s}/10^{12}\,{\rm G})^{0.7} \simeq (1.2\times 10^5\,{\rm K})b^{0.7}(P\dot{P}_{-15})^{0.36} \approx 10^6\,{\rm K}(B_{\rm s}/B_{\rm q})^{0.7}, \quad (3)$$

above which the thermionic ion flow reaches the maximum GJ density, thus screening completely any acceleration potential drop above the polar cap, where b, $B_{\rm s}$ and $B_{\rm q}$ are explained earlier in the paper. Below this temperature the charge-depleted acceleration region will form, that should most likely discharge in a quasi-steady manner by a number of sparks, as originally proposed by RS75 (see more detailed discussion in GMG03). The electron-positron plasma produced by sparking discharges co-exists with thermally ejected ions, whose charge density can be characterized by the shielding factor in the form $\eta = 1 - \exp[30(1 - T_i/T_{\rm s})]$. At the temperature $T_i = T_{\rm s}$ the shielding factor $\eta = 0$ (corresponding to fully developed space-charge limited flow with $\rho_i = \rho_{\rm GJ}$), but even a very small drop of $T_{\rm s}$ below T_i, much smaller than 10%, corresponds to creation of the pure vacuum gap with $\eta = 1$ ($\rho_i = 0$). Thus, the condition for partially screened charge depleted acceleration region can be written in the form $T_{\rm s} \lesssim T_i$, meaning that the actual surface temperature $T_{\rm s}$ should be slightly lower (few percent) than the critical ion temperature T_i, which

for a given pulsar is determined purely by the surface magnetic field $B_{\rm s}$. Although, the pure vacuum gap of RS75 is inconsistent with X-ray observations of drifting subpulse pulsar B0943+10 (see ZSP05), the condition for existence of the inner acceleration region can be used in a practical form

$$T_{\rm s} = T_i, \tag{4}$$

remembering that in reality $T_{\rm s}$ cannot be exactly equal to T_i (pure VG) but slightly (few percent) lower (partially screened gap).

As mentioned above, the polar cap surface can be negatively charged ($\boldsymbol{\Omega}\cdot\boldsymbol{B} > 0$). In such a case (called "antipulsars" by RS75) the polar cap surface can deliver an electron flow. Following GMG03 we assume that this electron flow is also determined mainly by thermo-emission, with a corresponding shielding factor $\eta = 1 - \rho_{\rm e}/\rho_{\rm GJ} = 1 - \exp[25(1 - T_{\rm e}/T_{\rm s})]$, where $\rho_{\rm e}$ is the charge density of thermionic electrons. The critical electron temperature

$$T_{\rm e} \simeq (5.9\times10^5\,{\rm K}) b^{0.4} P^{0.16} \dot{P}_{-15}^{0.2} \approx (2\times10^6\,{\rm K})(B_{\rm s}/B_{\rm q})^{0.4} \tag{5}$$

(see GMG03 for more details), and in analogy to Equation (4) the condition for creation of charge depleted acceleration region is $T_{\rm s} = T_{\rm e}$. This will be referred as to the "electron case" in the following discussion, in order to distinguish it from the "ion case" discussed above. We introduced the parameter $B_{\rm s}/B_{\rm q}$ for a convenience of presenting results in a graphical form (Fig. 1).

4 THERMOSTATIC REGULATION OF SURFACE TEMPERATURE

GMG03 argued (following the original suggestion by Cheng & Ruderman 1980), that because of the exponential sensitivity of the accelerating potential drop ΔV to the surface temperature $T_{\rm s}$, the actual potential drop should be thermostatically regulated at a temperature close to the critical temperature T_i or $T_{\rm e}$. In fact, when ΔV is large enough to ignite the avalanche pair production, then the backflow relativistic charges will deposit their kinetic energy in the polar cap surface and heat it at a predictable rate. This heating will induce thermionic emission from the surface, which will in turn decrease the potential drop that caused the thermionic emission in the first place. As a result of these two oppositely directed tendencies, the quasi-equilibrium state should be established, in which heating due to electron bombardment is balanced by cooling due to thermal radiation (see GMG03 for more details). This should occur at a temperature $T_{\rm s}$ slightly lower than T_i.

The quasi-equilibrium condition is $Q_{\rm cool} = Q_{\rm heat}$, where $Q_{\rm cool} = \sigma T_{\rm s}^4$ is a cooling power surface density by thermal radiation from the polar cap surface and $Q_{\rm heat} = \gamma m_{\rm e} c^3 n$ is heating power surface density due to back-flow bombardment, $\gamma = e\Delta V/m_{\rm e}c^2$ is the Lorentz factor and ΔV is the accelerating potential drop, $n = n_{\rm GJ} - n_i = \eta n_{\rm GJ}$ is the charge number density of back-flow particles that actually heat the polar cap surface, η is the shielding factor, n_i is the charge number density of thermally ejected flow and $n_{\rm GJ} = \rho_{\rm GJ}/e = 1.4\times10^{11} b \dot{P}_{-15}^{0.5} P^{-0.5}{\rm cm}^{-3}$ is the corotational charge number density. It is straightforward to obtain an expression for the quasi-equilibrium surface temperature in the form

$$T_{\rm s} = (1.98\times10^6\,{\rm K})(\dot{P}_{-15}/P)^{1/4}\eta^{1/2} b^{1/2} h_3^{1/2}, \tag{6}$$

where $h_3 = h/10^3$ cm is the normalized height of the acceleration region (Eqs. [1] or [2]). As a result of thermostatic regulation described above, this temperature should be very close to but slightly lower than the critical ion T_i or electron $T_{\rm e}$ temperature (Eqs. (3), (4) and (5)).

The X-ray thermal luminocity $L_x = \sigma T_{\rm s}^4 \pi r_{\rm p}^2 = 1.2\times10^{32}(\dot{P}_{-15}/P^3)(\eta h/r_{\rm p})^2$ erg s^{-1}, where $r_{\rm p} = 1.45\times10^4 b^{-1/2} P^{-1/2}$ cm is the actual polar cap radius. This X-ray luminosity can be compared with the spin-down power $\dot{E} = I\Omega\dot{\Omega} = 3.95\times10^{31}\dot{P}_{-15}/P^3$ erg s^{-1}. For the pulsar in which the tertiary circulational periodicity of drifting subpulses $\hat{P}_3 = NP_3$ (RS75) is known, where P_3 is a basic subpulse drift periodicity and N is a number of circulating subbbeams (Deshpande & Rankin 1999, 2001; Gil & Sendyk 2003), one can derive a relationship between observable and physical parameters of the partially screened acceleration region in the form

$$\eta h/r_{\rm p} \approx P/\hat{P}_3 \tag{7}$$

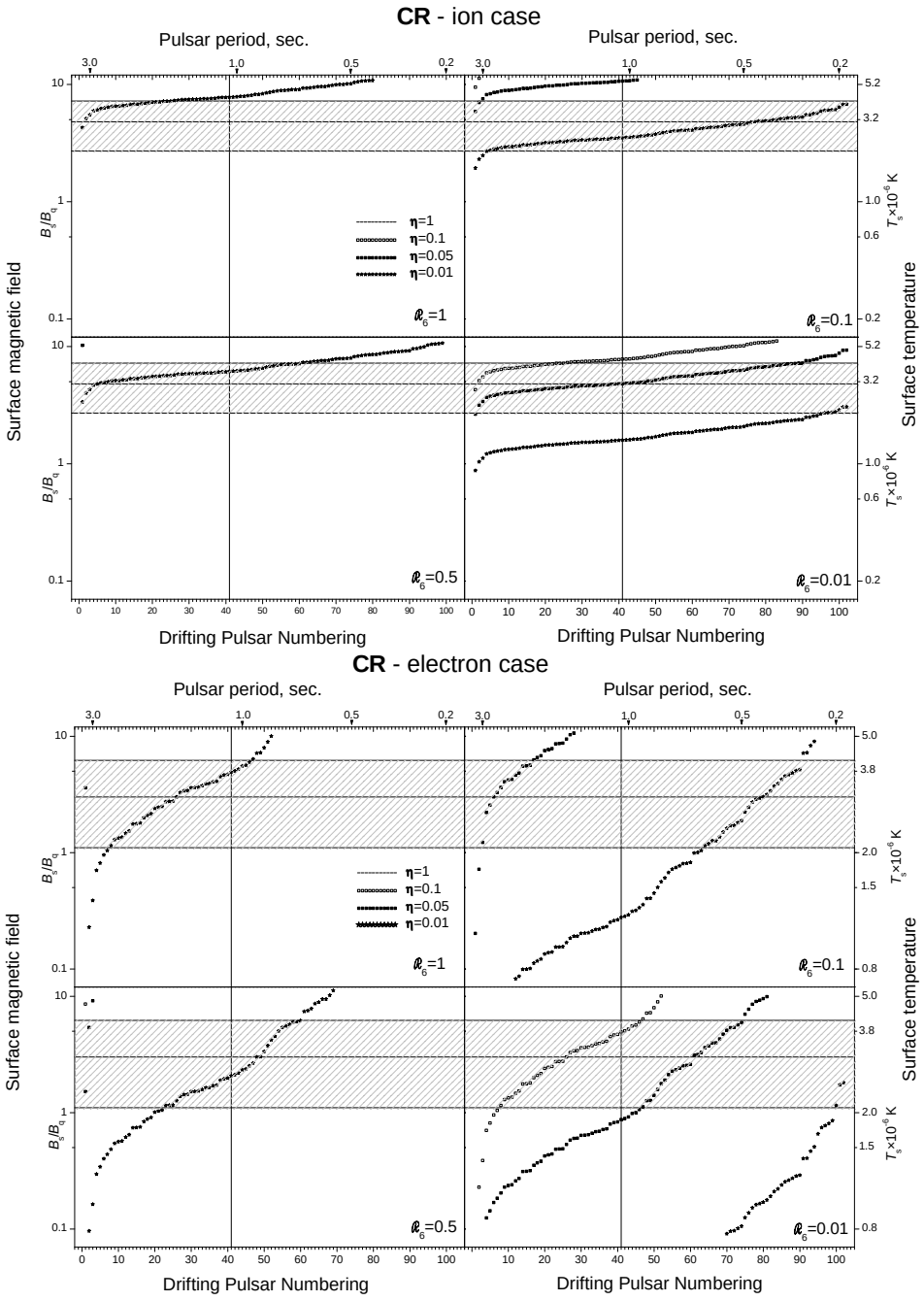

Fig. 1 Models of partially screened inner acceleration regions (see text for explanations).

(GMG03, ZSP05). We can now write an equation for the thermal X-ray luminosity from the heated polar cap

$$L_x \approx 3 \times 10^{31} (\dot{P}_{-15}/P^3)(P/\hat{P}_3)^2, \tag{8}$$

which depends only on the observational data of the radio pulsar. It is particularly interesting and important that this equation does not depend on details of the sparking gap model (η, b, h), which results from Equation (7) relating physical parameters of the acceleration region with the observational properties of

drifting subpulses. Thus, the Equation (7) describes a very neat relationship between properties of spark-associated drifting subpulses observed in radio band and characteristics of X-ray thermal radiation from the polar cap heated by sparks. For PSR B0943+10 with P=1.097 s and $\dot{P}_{-15} = 3.72$, which is the only pulsar for which both $\hat{P}_3 = 37.4$ P (DR99, DR01) and $L_x \approx 5 \times 10^{28}$ erg s^{-1} (ZSP05) is measured, the above equation is perfectly satisfied. Naturally, the efficiency $L_x/\dot{E} \approx 0.76(\hat{P}_3/P)^{-2} = 5.4 \times 10^{-4}$ is also perfectly satisfied in PSR B0943+10, for which the observational value $L_x/\dot{E} = 5 \times 10^{-4}$ (ZSP05). It should be mentioned that the thermal fit suggests that the emitting area is about $1^{+4}_{-0.4} \times 10^7$ cm^2. Even the largest area allowed by the fit is much smaller than the conventional polar cap area for a dipole magnetic field 6×10^8 cm^2 (ZSP05). Consequently $b \sim 60$ for this pulsar. In a few cases for which the circulational periodicity could be measured or estimated $14 < \hat{P}_3/P < 37$, thus generally $L_x/\dot{E} \sim (1^{+4}_{-0.5}) \times 10^{-3}$. Such correlation between X-ray and spin-down luminosities is well known and intriguing property of rotation powered pulsars (Becker & Trümper 1997; Possenti et al. 2002). It is believed that this correlation is a characteristic of a magnetospheric radiation (e.g. Cheng, Gil & Zhang 1998; Zhang & Harding 2000). Here we suggest that this can be also a characteristic property of the polar cap thermal radiation. Most likely, both mechanisms contribute in a comparable amount to the observed X-ray luminosity.

5 MODELS OF PARTIALLY SCREENED NEAR THRESHOLD GAP

Let us first consider curvature radiation dominated models of partially screened near threshold gap (CR-NTPSG). The results of model calculations for 102 pulsars with drifting subpulses (see Table 1) are presented in Figure 1. Two cases corresponding to the ion T_i (upper panel) and the electron $T_{\rm e}$ (lower panel) critical temperature are presented. Both panels correspond to quasi-steady discharge of the accelerating potential drop by cascading production of the electron-positron pairs driven (or at least dominated) by the curvature radiation seed photons. Pulsars were sorted according to decreasing value of the pulsar period P. We have then plotted $B_{\rm s}/B_{\rm q}$ (left-hand side vertical axes) versus the pulsar number (which corresponds to a particular pulsar according to Table 1), where $B_{\rm s} = bB_{\rm d}$ and $B_{\rm q} = 4.414 \times 10^{13}$ G is the so called quantum magnetic field. The actual value of $B_{\rm s}/B_{\rm q} = 0.045b(P \times \dot{P}_{-15})^{0.5}$ for a given pulsar was computed from the condition $T_{\rm s} = T_c$ (i.e.) $T_{\rm s} = T_i$ for upper and $T_{\rm s} = T_{\rm e}$ for lower panel of Figure 1, where $T_{\rm s}$ is the actual surface temperature. The vertical axes on the right hand side are expressed in terms of the surface temperature $T_{\rm s}$ computed from Equations (3) and (5) for the upper panel (ion case) and lower panel (electron case), respectively. Different plots correspond to different normalized radius of curvature ranging from $\mathcal{R}_6 = 1$ to $\mathcal{R}_6 = 0.01$. Different symbols (described in the left upper panel) used to plot exemplary curves correspond to an arbitrarily chosen values of shielding factor $\eta = 1$, 0.1, 0.05 and 0.01, respectively (each curve thus represents the same shielding conditions η for all 102 pulsars considered). Note that the curve corresponding to pure vacuum gap ($\eta = 1$) does not fit into any panel for $B_{\rm s}/B_{\rm q}$ below 10, or $T_{\rm s}$ below 5 MK. This means that in realistic pulsars the shielding parameter $\eta \ll 1$. As for the surface magnetic field value $B_{\rm s} \sim B_{\rm q}$, which suggests that $b \gg 1$ for almost all cases. The observations support such an assumption (ZSP05).

The vertical lines in Figure 1 correspond to PSR B0943+10 (number 41), which was observed using XMM-Newton by ZSP05. Three horizontal lines correspond to $T_{\rm s}$ equal to 2, 3 and 4 MK (from bottom to the top), respectively, calculated from Equation (3) for the ion case and from Equation (5) for the electron case. Thus the hatched area encompassing these lines corresponds to the range of surface temperatures $T_{\rm s} = (3 \pm 1) \times 10^6$ K deduced observationally for the polar cap of B0943+10 from XMM-Newton observations (ZSP05, see their Fig. 1). Although, for a given pulsar the charge depleted acceleration region can form at any $B_{\rm s}$ allowed by the condition $T_{\rm s} = T_c$ (i.e. $T_{\rm s} = T_i$ in the ion case or $T_{\rm s} = T_{\rm e}$ in the electron case), we know that in B0943+10 the surface temperature $T_{\rm s}$ is about 3 MK (ZSP05), which implies $B_{\rm s} = bB_{\rm d} \sim 2 \times 10^{14}$ G.

Analysis of Figure 1 shows that in the CR dominated ion case, a partially screened charge depleted acceleration region can form for all pulsars from Table 1. As one can see, the shielding factor η should be much smaller than 1.0 (perhaps even well below 0.1), otherwise the required surface magnetic field would be unrealistically high (exceeding 10^{15} G). Also, the larger values of the radius of curvature $\mathcal{R}_6$ correspond to smaller values of the shielding factor η. The values $\mathcal{R}_6 \gtrsim 0.5$ seem disfavoured. Realistically, the required surface magnetic field extends from about $0.1B_{\rm q}$ to about $10B_{\rm q}$, which is the range used on the vertical

Table 1 List of 102 Pulsars with Drifting Subpulses Compiled from R86 and WES05

Name	N	Name	N	Name	N	Name	N	Name	N
B0011+47	31	B0751+32	22	B1642–03	83	J1901–0906	12	B2043–04	18
B0031–07	49	B0809+74	27	J1650–1654	13	B1911–04	52	B2021+51	72
B0037+56	40	J0815+0939	63	B1702–19	91	B1914+13	93	B2044+15	38
B0052+51	6	B0818–13	32	B1717–29	64	J1916+0748	70	B2045–16	8
B0136+57	94	B0820+02	51	B1737+13	53	B1917+00	29	B2053+36	99
B0138+59	33	B0823+26	71	B1738–08	7	B1919+21	26	B2106+44	81
B0144+59	100	B0826–34	10	B1753+52	4	B1923+04	43	B2110+27	35
B0148–06	20	B0834+06	28	B1804–08	102	B1924+16	68	B2111+46	46
B0301+19	23	B0919+06	78	B1818–04	66	B1929+10	98	B2148+63	84
B0320+39	3	B0940+16	42	B1819–22	9	B1933+16	86	B2154+40	19
B0329+54	59	B0943+10	41	B1822–09	54	B1937–26	82	B2255+58	85
B0450+55	90	B1039–19	24	J1830–1135	1	B1942–00	44	B2303+30	17
B0523+11	87	B1112+50	14	B1839+56	15	B1944+17	77	B2310+42	88
B0525+21	2	B1133+16	36	B1839–04	11	B1946+35	58	B2319+60	5
B0540+23	95	B1237+25	25	B1841–04	47	B1952+29	79	B2324+60	96
B0609+37	92	B1508+55	56	B1844–04	67	B1953+50	73	B2327–20	16
B0621–04	45	B1530+27	39	B1845–01	61	B2000+40	50	J2346–0609	37
B0626+24	75	B1540–06	60	B1846–06	21	J2007+0912	76	B2351+61	48
B0628–28	30	B1541+09	55	B1857–26	65	B2011+38	97		
B0727–18	74	B1604–00	80	B1859+03	62	B2016+28	69		
B0740–28	101	B1612+07	34	B1900+01	57	B2020+28	89		

scale. Although the upper range values exceeding 10^{14} G may seem very high, one should realize that there are at least three pulsars which have dipolar magnetic fields above 10^{14} G (McLaughlin, Stairs & Kaspi 2003 and references therein), and the non-dipolar surface fields could be even stronger.

The upper panel of Figure 1 can be compared with the right-hand side of Figure 1 in GM02, where pure vacuum gap ($\eta = 1$) was considered. GM02 concluded that according to the binding energy calculations of J86 only ICS driven gap can form, while the CR driven gap could form only when the binding energies were much higher than those obtained by J86 (left-hand side of Fig. 1 in GM02), which is now believed highly unlikely (see Lai 2001). In this paper we demonstrated that in the presence of partial screening by thermal flow from the polar cap surface, the CR driven gap can form for all pulsars from Table 1 (and probably all pulsars with periods in the range $0.1\ \mathrm{s} < P < 6\ \mathrm{s}$).

The lower panel of Figure 1 is analogous to the upper panel, except it represents the electron case $T_\mathrm{s} = T_\mathrm{e}$. Analysis of these plots shows again that in the presence of significant thermal shielding ($\eta < 0.1$) the CR dominated charge depleted acceleration region can be formed for all pulsars from Table 1. Small values of $\mathcal{R}_6 \ll 0.1$ seem favored. Similarly to the ion case, the required surface temperature T_s is few MK.

Finally, let us consider the resonant inverse Compton scattering radiation (ICS) seed photon dominated models briefly (ICS-NTPSG). The major difference between CR and ICS cases is the additional regulation of T_s caused by the condition $h \approx l_\mathrm{e}$, where l_e is inversely proportional to T_s. In fact, the increase of the surface temperature causes decrease of h thus decrease of ΔV, which makes the back-flow heating of the polar cap surface less intense. Let us estimate the surface temperature in ICS dominated case. The average Lorentz factor of electrons or positrons can be estimated by the gap height and the partially screened potential drop as $\gamma = \left(1.1 \times 10^2\right) P^{1/6} P_\mathrm{dot}^{-1/6} b^{1/3} T_6^{2/3} \eta^{-1/3}$. Combining the kinematic near threshold condition and the expression for the resonant ICS photons energy (see section 2) we get $\hbar\omega = (7.5 \times 10^{-8}) \gamma b (P\dot{P}_{-15})^{-1/2}$, which leads to another estimate for an average Lorentz factors $\gamma = 2.5 T_6^{1/3} R_6^{1/3}$. Combining the two expressions for γ we find out that in the case of the ICS dominated NT-PSG the following relation should hold $\eta = 8.14 \times 10^{-5} P^{1/2} \dot{P}_{-15}^{-1/2} b T_6 \mathcal{R}_6^{-1}$. Thus, contrary to the CR case, in the ICS case η is not a free parameter, and the analysis similar to that presented in Figure 1 is not possible. However, we can use the quasi-equilibrium condition $\sigma T_\mathrm{s}^4 = \gamma m_\mathrm{e} c^3 n_0 \eta$, which leads to $T_6 = (8.8 \times 10^{-2})(\gamma \eta b P^{-3/2} \dot{P}_{-15}^{-1/2})^{1/4}$. Then using expressions for η and γ we obtain:

$$T_6 = 0.015 \mathcal{R}_6^{-1/4} P^{-3/8} \dot{P}_{-15}^{-3/8} b^{3/4}. \tag{9}$$

Consequently, we can obtain the expression for the shielding factor

$$\eta = \left(1.2 \times 10^{-6}\right) P^{1/8} \dot{P}_{-15}^{-7/8} \mathcal{R}_6^{-5/4} b^{7/4}. \tag{10}$$

Thus, for a given pulsar $(P, \dot{P})$ the values of $T_{\rm s}$ and η are determined by the parameters of the local surface magnetic field $\mathcal{R}_6$ and b. One can show (we can not present detailed analysis because of a lack of space) that Equations (9) and (10) cannot be self-consistently satisfied. In fact, typically $T_{\rm s} = T_6 \times 10^6$ K (Eq. (9)) is considerably lower than T_i (Eq. (3)) or $T_{\rm e}$ (Eq. (5)). This implies $\eta = 1$, which is impossible to get in general (Eq. (10)).

Acknowledgements We acknowledge the support of the Polish State Committee for scientific research under Grant 2 P03D 029 26.

References

Becker W., Trümper J., 1997, A&A, 326, 682
Cheng A. F., Ruderman M. A., 1980, ApJ, 235, 576
Cheng K. S., Gil J., Zhang L., 1998, ApJ, 493, L35
Deshpande A. A., Rankin J. M., 1999, ApJ, 524, 1008
Deshpande A. A., Rankin J. M., 2001, MNRAS, 322, 438
Gil J., Melikidze G. I., 2002, ApJ, 577, 909
Gil J., Melikidze G. I., Geppert U., 2003, A&A, 407, 315
Gil J., Mitra D., 2001, ApJ, 550, 383
Gil J., Sendyk M., 2000, ApJ, 541, 351
Gil J., Sendyk M., 2003, ApJ, 585
Goldreich P., Julian H., 1969, ApJ, 157, 869
Jones P. B., 1986, MNRAS, 218, 477
Lai D., 2001, Rev. Mod. Phys., 73, 629
McLaughlin M. A., Stairs I. H., Kaspi V. M. et al., 2003, ApJ, 591, L135
Possenti A., Cerratto R., Colpi M. et al., 2002, A&A, 387, 993
Rankin J. M., 1986, ApJ, 301, 901
Ruderman M. A., Sutherland P. G., 1975, ApJ, 196, 51
Urpin V., Gil J., 2004, A&A, 415, 356
Weltevrede P., Edwards R. I., Stappers B. A., 2006, A&A, 445, 243
Zhang B., Harding A., 2000, ApJ, 532, 1150
Zhang B., Harding A., Muslimov A., 2000, ApJ, 531, L135
Zhang B., Sanwal D., Pavlov G. G., 2005, ApJ, 624, L109